The UAV-based Test Source as an End-to-End Verification Tool for Aperture Arrays

F. Paonessa[1], G. Virone[1], P. Bolli[2], G. Pupillo[3], J. Monari[3], F. Perini[3], A. Mattana[3], G. Naldi[3], M. Poloni[3], M. Schiaffino[3], A. M. Lingua[4], M. Piras[4], P. Dabove[4], I. Aicardi[4], G. Addamo[1], O. A. Peverini[1], R. Orta[1] and R. Tascone[1]

Abstract – **A UAV-mounted radio-frequency transmitter is proposed as a known reference field source to perform a set of functional tests on aperture arrays. The experimental results obtained on complete prototypes (end-to-end) and sub-assemblies provide good confidence on both amplitude and timing verification.**

1 INTRODUCTION

The Square Kilometer Array (SKA) represents the near future of radio astronomy [1]. Both the low- (50-350 MHz) and mid-frequency (500-1500 MHz) instruments (to be deployed in the first and second phase of the SKA construction) will be implemented as Aperture Arrays having hundreds of thousands digitally-beamformed elements. Owing to both the overall system size and complexity, the deployment and commissioning of the Aperture Arrays will require the use of innovative strategies in order to confirm the required performance in an efficient and cost-effective manner. The overall information chain includes both RF (antenna, Low Noise Amplifier, analogue signal transportation and conditioning) and digital (sampling, beam-forming and correlator) parts. In this paper, a UAV-mounted continuous-wave test source is proposed as a known reference signal to perform a set of basic tests at both sub-assembly and end-to-end levels. The same test source concept has been already used in [2] as an antenna pattern verification system and in [3] to perform the array calibration. In [3], aerial photogrammetry has also been used to measure the real element positions.
The UAV-mounted test source is briefly described in section 2. Amplitude and timing verifications strategies are instead reported in section 3 and 4, respectively.

2 UAV-MOUNTED TEST SOURCE

Recently, the authors developed a UAV-mounted far-field test source to characterize the radiation pattern of VHF/UHF antennas [2]. Other interesting implementations of this concept can be found in [4]-[6]. The flying artificial test source consists of a battery-powered micro-Unmanned Aerial Vehicle (UAV), equipped with a continuous-wave radio-frequency transmitter and a dipole antenna (Fig 1). The UAV performs a completely autonomous flight: take-off, a sequence of waypoints with specific source orientation and landing can be programmed according to the required scan strategy. The UAV position during the flight is measured with a Differential Global Navigation Satellite System (DGNSS) exploiting a Post Processed Kinematic (PPK) approach, which provides an accuracy of few centimeters.

Figure 1: UAV-based flying test source. The payload consists of a GNSS receiver, an RF generator and a dipole antenna.

3 AMPLITUDE VERIFICATION

The amplitude of the array element transfer function (i.e. magnitude of the Jones's matrix elements) is very important since it affects the array sensitivity performance. For this reason, an accurate verification of such a parameter is mandatory. The proposed approach and the associated error budget is presented in the framework of the verification of a dual-polarized Vivaldi antenna for the Sardinia Array Demonstrator (SAD) [7]. Such an antenna (shown in Fig. 2) is made of stainless steel and can operate from 50 to 450 MHz. The lower operative frequency of SAD is however 250 MHz owing to the significant Radio Frequency Interference on site.
The measured radiation patterns are already reported in [8]. In this example, the unknown quantity is the overall gain of the antenna-LNA assembly. In principle, the verification of such a parameter can be accomplished by means of anechoic chamber setups that can be calibrated using reference antennas.

[1] CNR, Institute of Electronics, Computer and Telecommunication Engineering, C.so Duca degli Abruzzi 24, 10129, Turin, Italy, e-mail: giuseppe.virone@ieiit.cnr.it, tel.: +39 011 0905431, fax: +39 011 0905429.
[2] INAF, Osservatorio Astrofisico di Arcetri, Largo Enrico Fermi 5, 50125, Firenze, Italy.
[3] INAF, Istituto di Radio Astronomia, Via Fiorentina 3513, 40059, Medicina (BO), Italy
[4] Politecnico di Torino, Dipartimento di Ingegneria dell'Ambiente del Territorio e delle Infrastrutture, C.so Duca degli Abruzzi 24, 10129 Torino, Italy

However, the low operative frequency would require very complex and expensive systems. The key-point of the proposed procedure is instead the possibility of performance verification on site at low-cost, with no additional infrastructures, taking into account the real installation condition i.e. presence of soil ground and adjacent elements.

Figure 2: Dual-polarized cavity-backed Vivaldi for the Sardinia Array Demonstrator (SAD). The surface is made of a stainless steel wire mesh.

The measurement setup consists of the UAV-based test source described in Section 2, hovering about 70 m above the Antenna-Under-Test (AUT) in order to satisfy the Far-Field condition. The continuous-wave RF signal transmitted by the source is received by the ground-based AUT and measured by a spectrum analyzer. Additional coaxial cables and bias-tees are inserted between the AUT and the analyzer. It should be noted that all the setup components contribute to the power level recorded by the spectrum analyzer. The complete list and the corresponding values at 350 MHz are shown in Table 1. The contributions labelled with B, C, D and G have been accurately characterized (before the measurement) by means of standard RF lab equipment. The contribution E is known from simulations. The path loss F is computed from the DGNSS measured distance between test source and AUT. The parameter of interest (AUT Gain including LNA) can be easily obtained as H=A-B+C+D-E+F+G [9],[10]. The estimated errors associated to each contribution are also shown in Table 1. The resulting error on the parameter of interest (RMS criterion) is ± 0.22 dB. This value is already acceptable in terms of commissioning performance verification. It should be noted that reference antennas could have been used in this case in order to calibrate the measurement system and consequently remove all the systematic errors in Table 1. However, a suitable antenna configuration whose performance is totally independent of the presence of underlying soil ground (especially at 50 MHz, the lower frequency of the SKA) has not been found yet.

		Value	Error (dB)
A	Rec. Power	-33.88 dBm	± 0.1
B	Transm. Power	-0.35 dBm	± 0.1
C	Ins. Loss (balun)	0.80 dB	± 0.1
D	Mismatch Loss (UAV dipole)	0.28 dB	± 0.007
E	Source Gain	5.68 dBi	± 0.1
F	Path Loss	59.46 dB	± 0.01
G	Cable Loss	9.06 dB	± 0.1
H	**AUT Gain**	**30.38 dBi**	**± 0.22**

Table 1: Antenna+LNA Gain estimation at 350 MHz.

The measured results are compared to simulations in Table 2. At 250 and 350 MHz, the discrepancies are very consistent with the error budget. The higher error values at 450 MHz are related to a non-complete characterization of the mismatch loss of the source antenna, such a parameter has been in fact extrapolated from data at lower frequencies.

Freq	Polariz.	Measured AUT Gain	Simulated AUT Gain	Δ
MHz		dBi	dBi	dB
250	A	31.55	31.56	-0.01
	B	31.54	31.56	-0.02
350	A	30.38	30.51	-0.13
	B	30.60	30.44	+0.16
450	A	29.18	30.02	-0.84
	B	29.55	29.94	-0.39

Table 2: Comparison between measurement and simulation.

Even if the antenna-LNA assembly has been only considered in this example, the same approach can be easily extended to the characterization of more elements of the information chain i.e. larger sub-assemblies including RF links and receivers.
It should be noted that the presented amplitude verification procedure is also related to the overall array calibration (see for example [3]). In particular, the presented formulation can be exploited to compute the error associated to the magnitude of the array element calibration coefficients.
Finally, from a strictly technical point-of-view, the use of a UAV-based test source flying on an aperture array can be exploited to rapidly verify the consistency of connections and cable routing.

4 TIMING VERIFICATION

One of the key-elements of an aperture array is the digital back-end unit. Such an equipment basically performs A/D conversion, frequency channelization (Polyphase Filter Bank) and complex weighting for each array element. The same unit also performs beam-forming and signal correlation in real time. A simple procedure to verify that the back-end time reference is consistent to the DGNSS one is presented in this section. Such a technique, which has been developed on the Medicina Array Demonstrator (MAD) [3], [7], can be considered as a basic end-to-end system test.

The geometry of the MAD array is shown in Fig. 3. It is a regular configuration of dual-polarized Vivaldi antennas with a 1.5 m spacing. The picture of the demonstrator is shown in Fig. 4.

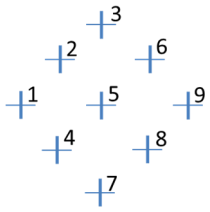

Figure 3: Geometry of Medicina Array Demonstrator. The element spacing is 1.5 m.

Figure 4: The Medicina Array Demonstrator with RF-over-fiber links (yellow cables).

The timing test has been accomplished with the UAV-mounted test source hovering at about 100 m over the array center. Figure 5 shows the position data measured with the DGNSS system. The origin of the reference system is located in the array center. The estimated precisions of 1.5 cm on the horizontal plane (X,Y) and 3.5 cm on the height (Z) are also shown. It is apparent that, during the observed 35 s timeframe, the test source is actually moving due to the lower accuracy (few meters) of the UAV navigation system. For this reason, the phase of the cross-correlation coefficient evaluated by the MAD back-end at 408 MHz is not constant with time (see Fig. 6). In particular, the parameter in Fig. 6 corresponds to the differential phase shift between the signals received by elements 3 and 7 (longest baseline, see Fig. 3). The blue and green curves represent the raw and averaged data (integration time 13.1 ms), respectively.

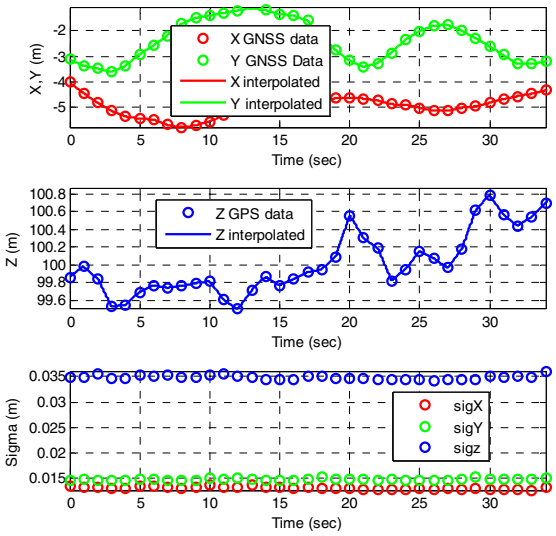

Figure 5: Measured position data when the UAV is hovering at about 100 m from the array center.

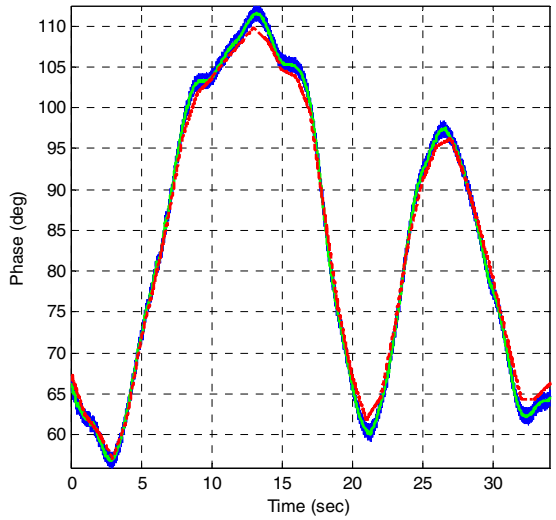

Figure 6: Phase shift between antenna 3 and 7 (longest baseline) at 408 MHz: measured raw-data (blue curve), averaged data (green curve), simulated data (red curve).

The measured behavior in Fig. 6 can be easily explained by computing the same parameter from the measured DGNSS data as $\varphi = K(R_3\text{-}R_7)$, where K is the propagation constant and R_3, R_7 are the distances between the test source and the two elements. Such a result is also reported in Fig. 6 (red curve). The average of the simulated curve (along the observed time window) has been aligned to the measured one in order to allow for a direct comparison. It appears that the data are in good agreement, the computed RMS discrepancy is about 1.25°. Besides the finite accuracy of the measured DGNSS data, such a discrepancy

could be due to a time shift between the DGNSS and MAD back-end time references even if both of them are supposed to time-stamp the data according to UTC time. The RMS discrepancy between measured and simulated phases resulting by artificially applying a time shift within ±1 s between the two data sets is shown in Fig. 7. The position of the minimum, which is very close to 0 s (-52.4 ms), confirms an acceptable alignment between the two data sets. According to the shape of the curve in Fig.7, which rapidly increases away from the minimum, it should be observed that the smallest detectable time shift could be very low. The minimum level is instead mainly related to the DGNSS precision [7].

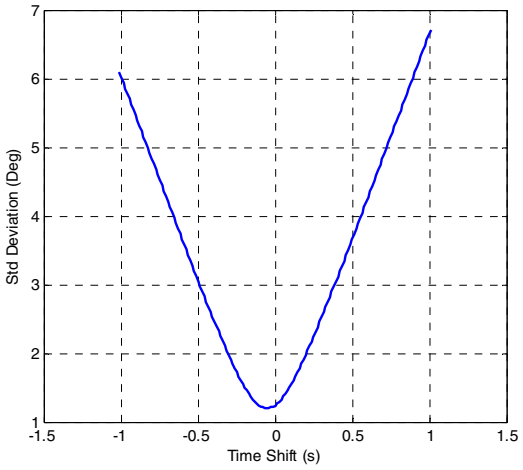

Figure 7: Evaluation of time shift between DGNSS and MAD digital back-end time references.

	Δϕ RMS No shift	Time Shift	Δϕ RMS Shifted
Baseline	Deg	ms	Deg
7 – 1	0.69	-78.6	0.60
7 – 2	0.74	-65.5	0.67
7 – 5	1.27	52.4	1.26
7 – 6	0.52	-13.1	0.52
7 – 9	0.47	-13.1	0.47
3 – 4	1.37	-65.5	1.33
3 – 8	1.49	-78.6	1.44
3 – 7	1.24	-52.4	1.20

Table 3: Measured and simulated RMS residual and estimated time-shifts of the cross-correlated data.

The same time shift estimation has been performed on the other measured baselines. The results are reported in Table 3 showing an overall dispersion of about 130 ms. Closer time shift values for all the baselines were instead expected according the initial assumption i.e. time shift phenomenon only related to the difference between the two time references. Further research work is hence required to understand the real source of such an observed data dispersion: more complex latency phenomena, the overall method accuracy or any other system component.

Acknowledgments

The authors would like to acknowledge the colleagues Paolo Maschio, Horea Bendea (DIATI, Politecnico di Torino) and Augusto Olivieri (CNR-IEIIT) for their valuable contribution to the experiments.

References

[1] www.skatelescope.org

[2] G. Virone, et al., "Antenna pattern verification system based on a micro unmanned aerial vehicle (UAV)," IEEE Antennas and Wireless Propagation Letters, vol.13, pp. 169-172, Jan. 2014.

[3] G. Pupillo, et al., "Medicina array demonstrator: calibration and radiation pattern characterization using a UAV-mounted radio-frequency source," Experimental Astronomy, vol. 39, pp. 405-421, Apr. 2015.

[4] F. Üstüner, et al. "Antenna Radiation Pattern Measurement Using an Unmanned Aerial Vehicle (UAV)", General Assembly and Scientific Symposium (URSI GASS), 2014 XXXI URSI, 16-23, Beijing. China, Aug. 2014

[5] A. Martínez Picar, et al. "Antenna Pattern Calibration of Radio Telescopes using an UAV-based device", International Conference on Electromagnetics in Advanced Applications (ICEAA), Sept. 7-11 2015, Turin, Italy.

[6] C. Chang, et al. "Beam Calibration of Radio Telescopes with Drones", Publications of the Astronomical Society of the Pacific, 127:000–000, November 2015.

[7] P. Bolli, et al. "From MAD to SAD: The Italian experience for the low-frequency aperture array of SKA1-LOW", Radio Sci., 51, 160–175, doi:10.1002/2015RS005922, Mar 2016.

[8] P. Bolli, et al., "Sardinia Aperture Array Demonstrator: Electromagnetic Analysis and Measurements," 36th ESA Antenna Workshop on Antennas and RF Systems for Space Science, Oct. 6-9 2015, Noordwijk, the Netherlands.

[9] G. Virone, et al., "Antenna pattern measurements with a flying far-field source (hexacopter)," IEEE International Conference on Antenna Measurements and Applications, Nov. 16-19 2014, Antibes Juan-les-Pins, France.

[10] P. Bolli, et al, "Antenna pattern characterization of the low-frequency receptor of LOFAR by means of an UAV-mounted artificial test source", SPIE Astronomical Telescopes and Instrumentation", Edinburgh, United Kingdom, 26 June - 1 July 2016